Eye (2021) 35:289–298
https://doi.org/10.1038/s41433-020-01188-0

The ROYAL COLLEGE of OPHTHALMOLOGISTS

ARTICLE

Blind patients in end-stage inherited retinal degeneration: multimodal imaging of candidates for artificial retinal prosthesis

Lorenzo Iuliano[1] · Giovanni Fogliato[1] · Eleonora Corbelli[1] · Francesco Bandello[1] · Marco Codenotti[1]

Received: 10 July 2020 / Revised: 11 September 2020 / Accepted: 14 September 2020 / Published online: 9 October 2020

Abstract

Purpose To characterize the imaging features of blind patients with end-stage inherited retinal degeneration (IRD) and to assess possible morpho-functional correlations.

Methods In this observational cross-sectional study, we reviewed the clinical data and multimodal imaging of 40 eyes of 21 blind (light perception or less) institutional patients affected by end-stage IRD screened for Alpha AMS (Retina Implant AG, Reutlingen, Germany) retinal prosthesis eligibility. Analysis was carried out using spectral-domain optical coherence tomography (SD-OCT), fluorescein angiography and fundus autofluorescence.

Results Among patients with IRD-related low vision, the extrapolated prevalence of the blind was roughly 10%, median age 60.4 years with a disease duration of 40.4 years, showing epiretinal membranes (80%), hyperreflective intraretinal nodules (90%) and the absence of the ellipsoid zone (77.5%) on SD-OCT examination. Cystoid macular oedema was present in 52.5% of eyes, the majority of which being of the microcystoid subtype (42.5%), while 37.5% of eyes also lacked outer and inner retinal layer segmentation. Disease duration was found to be predictive of disrupted retinal layers ($P = 0.029$) and microcystoid macular oedema ($P = 0.035$), which was also more frequent in eyes without light perception ($P = 0.013$).

Conclusions Eyes without vision due to end-stage IRD have a typical imaging pattern, predominantly characterized by epiretinal membranes, hyperreflective intraretinal nodules and the absence of the ellipsoid zone. Furthermore, microcystoid macular oedema and retinal layer disruption may be considered as signs of longstanding disease.

Introduction

Inherited retinal degeneration (IRD) includes a group of genetic retinal disorders of variable severity, among which retinitis pigmentosa (RP) is considered to be the most frequent and phenotypically representative. These disorders are estimated to be the most common cause of blindness in the working-age population, and in the past decade have exceeded the combined total of diabetic retinopathy and maculopathy [1].

The global median prevalence of RP is 1:4000 with the cumulative birth incidence at 27–80 cases every 100,000 live births [2]. The majority of these patients experiences progressive visual loss. Disease progression, expressed as half-life of the visual field, is ~7.3 years and can be measured using functional (e.g., microperimetry) and structural (e.g., optical coherence tomography and autofluorescence) surrogate marker [3].

Progression is unpredictable, as blindness in a small proportion of individuals might eventually be caused by photoreceptor degeneration and atrophy. The number of legally blind patients under 50 years of age is well below 10%, which rises to 20–25% for patients over 50 ("Retina Implant Surgeons Focus Group" conference in Frankfurt, February 2019, unpublished) [4, 5]. These rough data derive from expert and personal experience, and the exact proportion is still unknown.

In the last 10 years, several approaches have been used to treat IRD, including the promising gene replacement therapy [6–9], electrostimulation to delay progress in selected patients [10, 11], pharmacotherapy, stem-cell research, and optogenetics [12–14].

Supplementary information The online version of this article (https://doi.org/10.1038/s41433-020-01188-0) contains supplementary material, which is available to authorized users.

✉ Lorenzo Iuliano
iuliano.lorenzo@hsr.it

[1] Department of Ophthalmology, Vita-Salute University, San Raffaele Scientific Institute, Milan, Italy

Retinal implants are today the only available therapeutic option for end-stage RP patients. Subsuming the role of phototransduction, they have been seen to restore measurable vision in some blind patients, enabling object localization and rough-detail detection [15–19]. Only four devices have been granted CE marking for commercial use in the European Economic Area: Retina Implant Alpha IMS (first-generation device, Retina Implant AG, Reutlingen, Germany), Retina Implant Alpha AMS (second-generation device, Retina Implant AG), Argus II Retinal-Prosthesis System (Second Sight Medical Products Inc, Sylmar, CA), and IRIS II (Pixium Vision, Paris, France) [20, 21].

Retinal implant manufacturers and researchers both accept, however, that there is still a degree of uncertainty regarding those patients who might be suitable for these devices, as well as the perceived benefit on the part of users and experts.

Herein, we systematically analyzed the retinal characteristics of patients undergoing eligibility screening for Alpha AMS implant surgery at our centre with multimodal imaging. The recruited patients were all legally blind, and our investigation focused on the most neglected subgroup of RP patients that rarely undergo regular visits. The aim was to identify specific disease characteristics or patterns, as well as possible associations, in order to profile certain specific patient subtypes.

Methods

In this observational cross-sectional study, we selectively reviewed the electronic medical charts of blind patients affected by end-stage IRD, screened for Alpha AMS eligibility from July 2017 to December 2017.

Each procedure performed involving human participants was in accordance with the tenets of the 1964 Declaration of Helsinki and its later amendments. Our research was approved by the Institutional Review Board (IRB) of the San Raffaele Scientific Institute (approval number 102/INT/2017, protocol ALPHA-RET-1). All patients signed an informed consent form, which was specifically designed and approved for this protocol.

The Alpha AMS system

The key distinction between the Alpha AMS and the Argus II or IRIS II systems is that the first consists of a photodiode array located in the subretinal space (anatomic plane of the degenerate photoreceptors), whereas the others have an epiretinal array on the surface of the retina. Furthermore, the Alpha implant performs both light detection and charge transfer to the overlying inner retina, whereas the Argus II and IRIS II use a spectacle-mounted digital camera to detect incident light, which is then transmitted wirelessly to the implant receiver [21, 22].

Study protocol

The Public Relations Office of the San Raffaele Scientific Institute, following IRB approval, launched a campaign to recruit patients eligible for Alpha AMS artificial retina implantation.

The project was promoted through selected media and social channels, including the Blind & Low-vision Patients Union, dedicated patient associations and media services specializing in health and medicine. Patients, or their relatives, were invited to contact our department using a dedicated phone number and e-mail address to schedule remote evaluation with an expert ophthalmologist (LI, MC). Patients were initially screened to exclude any obviously ineligible individuals (e.g., those retaining useful vision, those who had lost vision due to causes other than IRD).

All presumably eligible patients were given an appointment at our centre, where they underwent complete clinical evaluation, including general and ocular medical history, family history of the disease, best-corrected visual acuity (BCVA), applanation tonometry, slit-lamp examination, fundus biomicroscopy, and multimodal imaging including fundus photography, infra-red reflectance, fundus autofluorescence (FAF), structural spectral-domain optical coherence tomography (SD-OCT), and fluorescein angiography (FA). Those fulfilling the inclusion criteria and judged eligible for Alpha AMS implantation were put on a waiting list for surgery.

In our analysis, we included all screened patients with visual acuity equal or inferior to light perception (LP), whose imaging and data concerning demographic and clinical characteristics were acquired from electronic medical charts.

Inclusion/exclusion criteria

All subjects were recruited at the Vitreoretinal Surgery Service of the Ophthalmology Department, San Raffaele Scientific Institute. In our study, we included all eyes that fulfilled the following inclusion criteria:

- IRD of the outer retinal layers
- Age between 18 and 78 years
- BCVA in the best eye from LP to no LP (NLP) [≥2.7 LogMAR [23]]
- Ability to read normal print in earlier life, optically corrected without magnifying glass

Exclusion criteria were as follows:

- Other retinal diseases (e.g., diabetic retinopathy, uveitis, retinal vein occlusion, retinal detachment, etc.)

- Optic nerve diseases (e.g., history of glaucoma, optic neuropathy that does not appear associated with IRD)
- Amblyopia reported earlier in life on eye to be implanted
- Period of appropriate visual function <12 years/lifetime
- Subjects whose imaging acquisition was jeopardized by optical media opacity (cornea or lens)

Fulfilment of these criteria did not automatically imply eligibility to receive Alpha AMS, as (per manufacturer's disposition) additional inclusion criteria also needed to be respected (Supplementary information—Table 1).

Investigated variables

All demographic and general clinical data were collected and analyzed. Axial length was measured using IOL Master 500 (Zeiss, Oberkochen, Germany).

All gradings were carried out by two independent graders (LI and GF). Inter-grader reliability was calculated for each measurement. Images with any level of disagreement were reviewed during live adjudication session. A third grader (MC) was on hand only for those cases where no agreement might be found.

Visual acuity

Ultra-low visual acuity was always tested in a dedicated dimly lit office by the same operator (EC), with stable and continuously monitored luminance (50 lux at the subject's eye). Each eye was tested using the Frieburg Visual Acuity Test (FrACT) [23–26].

The FrACT is a widely used visual test battery based on a computer programme that uses psychometric methods, combined with anti-aliasing and dithering, to provide automated, self-paced measurement of visual acuity [27]. A Landolt-E optotype appears on the screen and changes with each trial, as does its orientation, which is fully randomized. The subject is instructed to point in the perceived direction with a forced-choice strategy. The inbuilt software algorithm is structured to provide a higher number of optotype presentations near the patient's VA threshold [25, 26], and final visual acuity is expressed using 20/20 and LogMAR scales.

During the test, the subject sat 60 cm from a 24″ touch LED Monitor (Dell 24 Touch Monitor, Dell, Round Rock, TX, USA), used as an extension of the examiner's laptop. The FrACT was calibrated with a luminance of 250 cd/m^2 and a resolution of 1920 × 1080.

Subjects with a BCVA equal to or greater than 2.7 LogMAR, which might be estimated as LP [23, 24], were tested for LP. A routine clinical "hand motion" test was however used for confirmation, asking the patient to state the examiner's hand motion (horizontal, vertical, oblique) at 50 cm in a normally lit room. The test was carried out five times; LP status was confirmed in those unable to correctly recognize hand movement during each repetition.

Slit-lamp LP evaluation was carried out for each patient, using the chin and forehead rest in a dim environment with the fellow-eye patched. The light beam was directly projected onto each eye and reduced to the lowest level with the dimmer switch. After having adapted to the dark for 3 min, patients were asked to report the moment they perceived light as the dimmer switch was increased. The procedure was carried out twice per eye, and those failing to answer, or giving inadequate answers were graded as NLP.

Furthermore, eyes retaining LP were subjectively graded as follows: "unstructured LP" was assigned to patients claiming to see light sources with that eye, but who were unable to locate them in space or use them for navigation or orientation; "structured LP" was assigned to patients able to recognize and locate light sources in space, such as a window or a switched-on lamp.

The presence and degree of nystagmus was also recorded.

Spectral-domain optical coherence tomography

Structural SD-OCT macular region scans were performed using the Spectralis HRA + OCT system (Heidelberg Engineering, Heidelberg, Germany). The acquisition protocol included a six-line radial SD-OCT pattern (1024 A-scans per B-line scan) cantered on the fovea at a 30° distance. Central foveal thickness (CFT) was assessed in the central 1-mm-diameter circle of Early Treatment Diabetic Retinopathy Study thickness map using Spectralis Software (Heidelberg Eye Explorer 1.9.11.0, Heidelberg, Germany). Subfoveal choroidal thickness was measured manually as the distance between the Bruch's membrane interface and the sclero-choroidal interface under the fovea. Eye tracking was enabled during image acquisition to enhance image resolution. To achieve good visualization of the choroid, enhanced depth-imaging (EDI) OCT was used in acquisitions for choroidal evaluation.

For each eye, the following SD-OCT findings (Fig. 1) were specifically examined and graded:

- Epiretinal membrane, defined as a hyperreflective layer of fibrous tissue above the inner surface of the retina, was judged as absent or present
- Hyperreflective intraretinal nodules, defined as isolated round and discrete hyperreflective clumps right above and detached from the retinal pigment epithelium (RPE), were judged as present or absent
- Foveal atrophy, defined as the complete loss of retinal tissue in the foveolar area, was judged as absent or present

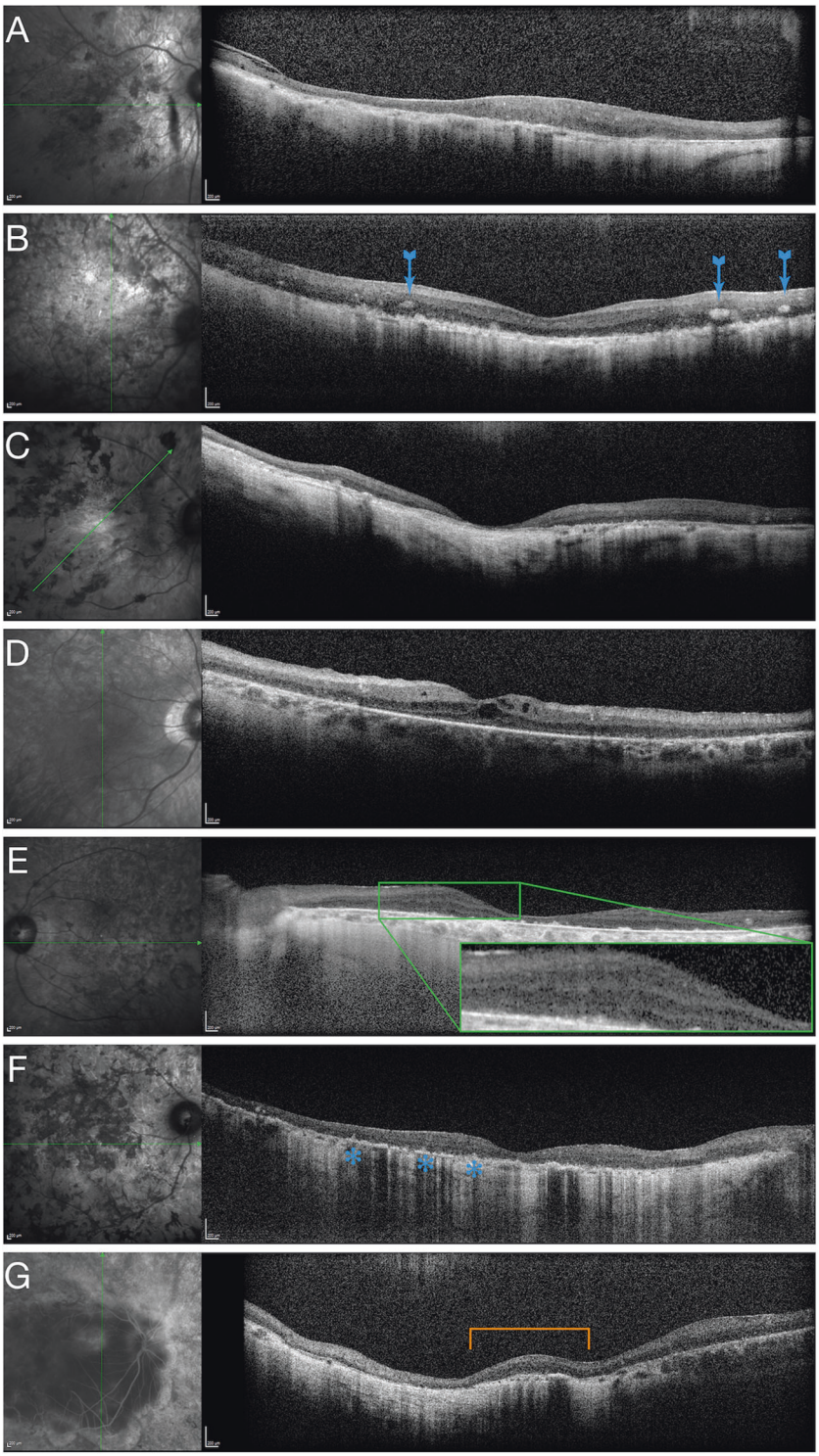

Fig. 1 Spectral-domain optical coherence tomography (SD-OCT) features of blind eyes affected by inherited retinal degeneration. The most frequent structural SD-OCT findings in blind RP patients were as follows: epiretinal membrane (**a**) and the hyperreflective intraretinal nodules (**b** blue arrows). Other features: foveal atrophy (**c**), cystoid macular oedema (**d**), microcystoid macular oedema (**e** with parafoveal magnification), retinal pigment epithelium clumps (**f** blue asterisks) and scleral bumps (**g** orange segment).

- Cystoid macular oedema (CMO), defined as hyporeflective cystoid spaces in any of the macular layers associated with retinal thickening, was judged as absent or present. If present, CMO was further subclassified into classic or microcystoid macular oedema (MMO), presenting as tiny discrete hyporeflective cysts usually confined to a single retinal layer (or two contiguous layers), with no leakage at the FA
- RPE clumps, defined as hyperreflective bumps under or in the context of the RPE, were judged as present or absent

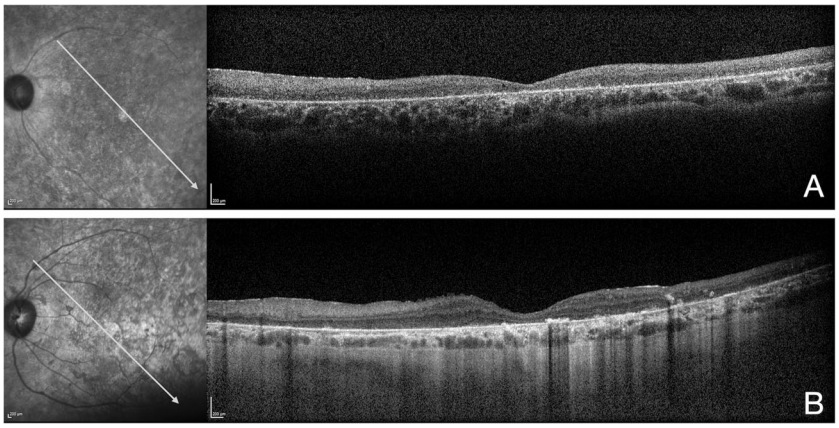

Fig. 2 Examples of different possible retinal layering at spectral-domain optical coherence tomography (SD-OCT) in blind eyes affected by inherited retinal degeneration. Scans **a** and **b** exemplify two cases of ill- and well-defined retinal SD-OCT layering. In **a** the retinal nerve fibre layer is the only defined layer, whereas the others are indistinguishable. In **b** intraretinal architecture is rather preserved.

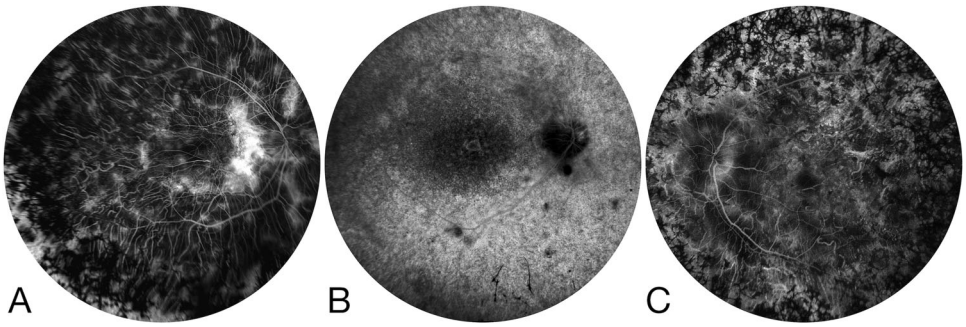

Fig. 3 Different fluorescein angiography patterns of blind eyes affected by inherited retinal degeneration. Angiogram **a** (3:02 min) serves as example of a well-vascularized posterior pole. Angiogram **b** (1:06 min) and **c** (2:59 min) are representative of a remarkably reduced vascularization, respectively in the macula and in the periphery.

- Scleral bumps, defined as bulging deformations of the scleral profile engendering a convex profile of the overlying choroid and retina
- Integrity of the retinal layers, that was defined according to the number and type of recognizable layers in all the structural scans centred on the macula. Considering the profound structural disorganization of the retinal layers in RP patients, layering was roughly divided into two stacked categories: (1) the retinal nerve fibre layer (RNFL); (2) the remaining retinal layers, namely the inner (including at least the ganglion cell layer, the inner plexiform layer of the inner nuclear layer) and the outer (including at least the outer plexiform layer of the outer nuclear layer). The graders were asked to evaluate if (1) was recognizable or not and if within (2) the outer and inner layers were distinct (Fig. 2)
- Ellipsoid zone (EZ) integrity that was judged as "intact" if continuous and hyperreflective "irregular" if discontinuous with iso- or hyporeflective tracts, or "absent" if completely unrecognizable

Fluorescein angiography

Angiograms were evaluated for:

- Vascular perfusion, judged respectively in the macula and in the periphery as absent in the case of a complete dearth of fluorescence of the capillary bed, or reduced if the fluorescein signal was present but attenuated (as expected in end-stage RP) (Fig. 3)
- Leakage, defined as the presence or absence of hyperfluorescent areas located along vessels, the optic nerve, or the macular area

Fundus autofluorescence

FAF was performed by exciting retinal pigments with blue light ($\lambda = 488$ nm) and was averaged for all scans. Images were graded as normal, advanced (widespread atrophy involving the fovea with decreased autofluorescence), or with the hyperautofluorescent ring that is characteristic of IRD.

Statistical analysis

Statistical analyses were carried out using GraphPad Prism version 5.00 for Mac (GraphPad Software, San Diego, California, USA) and SPSS Statistics Version 20 (IBM, Armonk, New York, USA). Distribution normality was tested with Shapiro–Wilk test. Continuous variables were compared with *T* tests and with non-parametric ANOVA tests. The presence of statistical association was tested with the chi-square and the Fisher's test. Association of continuous variables was tested with binary logistic regression.

Table 1 Demographic characteristics of blind patients affected by inherited retinal degeneration.

	Years ± SD	Range	Median	Normal distribution
Age	60.4 ± 13.8	40–90	59	Yes
Age at diagnosis	20 ± 13.9	6–60	16	No
Disease duration	40.4 ± 16.3	10–72	39	Yes
Blindness duration	15.2 ± 8.2	2–30	15	Yes

SD standard deviation.

Inter-grader reliability for baseline values was calculated using intraclass correlation coefficients (ICC) based on a two-way random-effects model. In all analyses, P values < 0.05 were considered significant.

Results

During the recruitment period, 721 subjects contacted our centre through the dedicated channels. Of these, 326 were diagnosed with IRD, whereas the others had diseases such as end-stage diabetic retinopathy, trauma, optic neuropathy and retinal detachment. The most frequent reported diagnosis was RP (201 subjects, 61%), followed by Stargardt disease (97 subjects, 30%), generic "tapetoretinal dystrophy" (19 subjects, 6%) and cone-rod dystrophy (9 subjects, 3%).

Those who claimed to be blind, or were certified as being legally blind, were offered an appointment. Each of the 40 contacted patients accepted and was scheduled for a visit. In our analysis, we did not consider six subjects, five of whom with a BCVA of hand motion and one of counting fingers.

Patients with BCVA ≤ LP were therefore 10.4% (34 subjects) of the whole sample that contacted our centre with a diagnosis of IRD and low vision. Of these, we enroled 21 (40 eyes) that respected the study inclusion/exclusion criteria. Two eyes of two patients had cloudy media and were not considered.

All included patients had a diagnosis of RP, of which 19 were typical RP and two syndromic RP: one Usher syndrome type-1 and one Bardet–Biedl syndrome. Female to male ratio was 6:15. Demographic characteristics are shown in Table 1. Blindness duration was calculated according to the estimated time referred by each subject since vision had deteriorated to LP or less.

Two patients (9.5%) had large-amplitude nystagmus, while 12 (57.1%) showed intermittent and small-amplitude nystagmus.

Of the 40 included eyes, 11 (27.5%) were pseudophakic. The other 29 eyes (72.5%) showed a cataract, 20 of which (50%) of the posterior subcapsular subtype. Average axial length was 24.89 ± 0.12 mm (range 23.99–26.81 mm).

Ten eyes (25%) had NLP, 12 (30%) had unstructured LP, and 18 (45%) had structured LP.

Table 2 Relative frequencies of the spectral-domain optical coherence tomography findings in blind eyes affected by inherited retinal degeneration.

	Frequency % (*n*)	ICC	95% Confidence interval
Epiretinal membrane	80 (32)	0.8602	0.7519–0.9234
Hyperreflective intraretinal nodules	90 (36)	0.9103	0.8378–0–9514
Foveal atrophy	27.5 (11)	0.8836	0.7905–0.9367
Cystoid macular oedema	52.5 (21)	0.7588	0.5883–0.8647
Microcystoid macular oedema	*42.5 (17)*	*0.9103*	*0.8378–0.9514*
RPE clumps	32.5 (13)	0.8304	0.7014–0–9067
Scleral bumps	20 (8)	0.9103	0.8378–0.9514
Ellipsoid zone			
Intact	0	1	1–1
Irregular	17.5 (7)	0.9103	0.8378–0–9514
Absent	77.5 (31)	1	1–1

ICC intraclass correlation coefficient, *RPE* retinal pigment epithelium.
Italics was placed to represent the fact the percentage of Microcyistoid Macular Oedema is a subpart of the line Macular Oedema.

The frequency of SD-OCT findings can be found in Table 2. All variables disclosed high inter-rater agreement. Conflicting gradings were resolved after adjudication session, finding an agreement with the senior grader's (LI) readings. The third grader was never invoked.

The most frequent SD-OCT findings in blind RP patients were as follows: epiretinal membrane and hyperreflective intraretinal nodules. Macular oedema was present in almost 50% of eyes, the majority of which being MMO. One third of all eyes showed RPE clumps, while EZ was not found to be intact in any of the eyes, except in seven eyes, which was considered irregular.

Retinal layer integrity frequency is shown in Supplementary information—Fig. 1. Of note, in three eyes (7.5%) none of the layers was recognizable, while in 12 (30%) the RNFL was identifiable but the inner and outer layers were undistinguishable (Fig. 2). The inner and outer layers were recognizable in 25 (62.5%) eyes.

Average CFT was 68.2 ± 70.6 µm (range 0–275, median 57.5), while subfoveal choroidal thickness was 106.9 ±

98.8 µm (range 0–300, median 80), both without normal distribution.

Fluorescein angiography confirmed the typical picture of vessel narrowing and capillary rarefaction in the majority of eyes. Advanced signs were found in two eyes (5%), where we noted the absence of macular perfusion, and in three different eyes (7.5%), where peripheral absence of perfusion was highlighted. The two eyes with an absence of macular perfusion had macular atrophy. Perivascular leakage was found in one eye (2.5%).

Hyperautofluorescent halo at FAF was never identified in any of the investigated eyes. Each acquisition (100% of eyes) was judged as advanced.

Eyes were then grouped by visual function, dividing those retaining a somehow useful form of vision (structured LP) from those without (unstructured LP and NLP together). CFT was similarly distributed between structured LP (80.9 ± 70.5 µm) and unstructured LP/NLP (57.9 ± 70.6 µm; $P = 0.28$). Subfoveal choroidal thickness was likewise distributed, respectively. 118.0 ± 21.2 and 97.7 ± 106.8 µm; $P = 0.34$.

Autofluorescence and FA patterns were also similar between the two groups. Frequency analysis of the different SD-OCT features (Supplementary information—Table 2) found the proportion of MMO to be significantly higher in the unstructured LP/NLP group ($P = 0.013$).

Logistic regression analysis eventually highlighted that disease duration was predictive of the presence of MMO ($P = 0.035$). Longstanding RP was also predictive of the lack of segmentation, since disease duration was also correlated with the absence of outer/inner layer recognizability ($P = 0.029$). No other significant correlations were singularly found between disease duration, age, age at diagnosis, and blindness duration and any of the investigated variables.

Discussion

Retinal implants are today the only approved and available treatment option for end-stage IRD, and are likely to remain a relevant option for vision restoration in the foreseeable future. With ongoing technical development, patient training, and clinical improvement, the benefits that retinal implants provide can help improve the lives of patients.

Experts confirm that patients benefit, to varying degrees, from retinal devices [20, 21]. Functional outcome is, however, substantially variable, as the visual capacity of a number of eyes is not restored following prosthesis implantation, or else is enhanced to a level that remains below the patient threshold of visual perception. The reasons for this variability may be found in the remarkably different microenvironmental changes in visual pathway biology.

The primary defect of IRD, particularly of RP, is found in the rod photoreceptors, which eventually die. Consequent cone cell death follows, presumably due to oxidative damage and starvation [28, 29]. Although damage is initially triggered in the photoreceptors, degenerative processes progressively spread to the neural retinal connections (bipolar and ganglion cells), leading to a gradual loss of function and to measurable anatomic atrophic changes.

This crucial aspect might account for those cases where implants, despite technological proof of correct functioning, seem not to work properly. Retinal prostheses can indeed replace the role of photoreceptors (phototransduction), delivering a bioelectrical stimulus to a retinal neural network, the functional status of which we do not fully understand. The paradigm of the "retinal prosthesis" should hence be remodelled to the "photoreceptor prosthesis".

In vivo assessment of the functional status of retinal connections might offer clinicians a powerful tool to select, from those who are eligible, the most suitable candidate for a retinal prosthesis.

Our study did not aim to answer this demanding question; it was designed to better characterize the blind segment of patients with IRD, taking advantage of the screening procedure performed at our centre to find eligible patients for Alpha AMS subretinal implantation.

Our study selectively focused on patients with extremely low vision, from LP to no LP. The cohort of patients that contacted our centre might be considered representative of those with IRD and very low vision. The proportion of blind patients (≤LP) extrapolated from this cohort was roughly 10%, which is consistent with data deriving from expert experience ("Retina Implant Surgeons Focus Group" conference in Frankfurt, February 2019, unpublished) [4, 5]. Average age (60 years) was also coherent with a long history of disease of over 40 years.

Demographic data are in agreement with disease epidemiological characteristics, such as the presence of cataract in 100% of eyes (including pseudophakic) [30].

Structural SD-OCT analysis showed that the clinical characteristics found in blind eyes, the most frequent findings being epiretinal membrane and hyperreflective intraretinal nodules. While the first has already been extensively reported [31], the second might represent a sign of intraretinal pigment or RPE migration [32, 33].

The EZ, which has already been described as being significantly associated with and predictive of visual function in RP eyes [34–38], was understandably never found intact in our sample, and was, indeed, completely absent in 77.5% of cases. It might thus be considered a hallmark of blind eyes.

The lack of retinal layer segmentation can also be included in the SD-OCT patterns of advanced RP eyes, which has already been described [39]. Owing to profound

retinal layering disorganization, we waived singular evaluation of any of the retinal layers. We simplified segmentation assessment by grading it as the presence of RNFL and the recognizability of outer/inner layers. We found that inner/outer layers were not even distinguishable in more than one third of the eyes (37.5%). We assumed that degenerative cellular changes alter tissue reflectivity to make layer texture similar.

CMO was present in almost half of the eyes examined, the majority of which was of the microcystoid subtype. Macular oedema is unanimously considered to be a characteristic of the disease [35], as well as MMO. This oedema subtype, reported by other researchers as micropseudocysts [31] and described also in eyes with glaucoma [40], is not related to retinal vascular impairment, and its determinants include the trans-synaptic degeneration of inner retinal layers. MMO is said to be caused by retrograde degeneration of the inner retinal layers, resulting in impaired fluid resorption in the macula [40–43]. Since in RP degenerative processes ultimately spread to the inner layers, this sign may be consistent with longstanding RP.

Other signs, observed in nearly one third of the eyes, were RPE clumps, a non-specific sign of RPE atrophic changes [44, 45], and foveal atrophy, which shows further agreement with the remarkably reduced CFT we found in the eyes examined.

Finally, we hypothesized that scleral bumps, present in one fourth of the eyes, can be encompassed in end-stage scarring changes of the choroid and its external scleral interface.

Fluorescein angiography and autofluorescence eventually confirmed the advanced-stage features in those eyes, without adding strikingly unique characteristics.

In the attempt to associate any possible morpho-functional trait to blind RP eyes, we divided the eyes retaining some useful form of vision (structured LP) from those without (unstructured LP and NLP together). We found that all the SD-OCT, FA and FAF features were similarly distributed between the two groups, except for MMO that was significantly more represented in the group of eyes without structured vision or with an absence of vision. This might further confirm the retrograde neurodegenerative significance of MMO, which we speculate could be more represented in eyes without vision.

Furthermore, logistic regression analysis supported this evidence, highlighting how disease duration was predictive of MMO presence. The longer the disease is present, the higher is the chance of having MMO with, moreover, retinal layer disruption.

This study has important limitations that should be taken into account. First, owing to its cross-sectional design, it lacks any longitudinal consideration. Second, we did not have the opportunity to group patients according to inheritance pattern, or to argue any genotype–phenotype considerations. Third, our statistical data are biased by the fact that we accounted each eye singularly rather than as a couple. Extrapolated prevalence should be considered with caution, as patients with near-normal vision might have been discouraged from contacting the clinic.

However, our research also has numerous strengths. First, it included a representative set of eyes from a segment of patients that is usually neglected at routine ophthalmological visits. Second, strict and accurate inclusion criteria made our sample representative. Third, subjective evaluation disclosed high inter-rater agreement.

A final consideration concerns the regulatory definitions of blindness. Italian law n.138/2001 defines as being "totally blind" those who completely lack the vision of light in both eyes, those who retain the mere vision of light or hand motion in the best eye, and those whose perimetric residual is inferior to 3%. We emphasize that not all the individuals included in this definition may be eligible for retinal prostheses. It might therefore be misleading to claim that retinal implantation is suitable for "totally blind" subjects.

In conclusion, we believe that this study provides ophthalmologists with a solid clinical definition of the imaging features of blind eyes for IRD. It might also lay the foundations for the knowledge of morpho-functional correlations, as it sheds light on signs that might be considered predictive of disease duration. These data may be of help to better define the patient profile of subjects retaining a structurally preserved retinal connection. Eventually these data, correlated with those from the outcome after future implantations, might help identify the ideal candidate that could benefit from an artificial retina.

Forthcoming empowered research might offer unique hallmarks (through imaging or electrophysiology) of retinal neural network integrity. This might finally give clinicians the opportunity to offer blind patients retinal-prosthesis treatment with realistic expectations of success.

Summary

What was known before

- There is a degree of uncertainty regarding the proportion and the characteristics of patients with inherited retinal degenerations who might be suitable for retinal prostheses.

What this study adds

- Among patients with inherited retinal degenerations, the extrapolated prevalence of the blind is roughly 10%.

- Eyes without vision have a characteristic imaging pattern.
- Some specific imaging features are related to the residual visual status and may be suggestive of the disease duration.

Acknowledgements The authors thank Michael John of the Vita-Salute University for the English language editing of this paper.

Compliance with ethical standards

Conflict of interest LI, GF, EC and MC: none. FB reports personal fees from Alcon (Fort Worth, TX, USA), personal fees from Alimera Sciences (Alpharetta, GA, USA), personal fees from Allergan Inc (Irvine, CA, USA), personal fees from Farmila-Thea (Clermont-Ferrand, France), personal fees from Bayer Shering-Pharma (Berlin, Germany), personal fees from Bausch And Lomb (Rochester, NY, USA), personal fees from Genentech (San Francisco, CA, USA), personal fees from Hoffmann-La-Roche (Basel, Switzerland), personal fees from NovagaliPharma (Évry, France), personal fees from Novartis (Basel, Switzerland), personal fees from Sanofi-Aventis (Paris, France), personal fees from Thrombogenics (Heverlee,Belgium), personal fees from Zeiss (Dublin, USA), outside the submitted work.

References

1. Liew G, Michaelides M, Bunce C. A comparison of the causes of blindness certifications in England and Wales in working age adults (16-64 years), 1999-2000 with 2009-2010. BMJ Open. 2014;4:e004015.
2. Ferrari S, Di Iorio E, Barbaro V, Ponzin D, Sorrentino FS, Parmeggiani F. Retinitis pigmentosa: genes and disease mechanisms. Curr Genom. 2011;12:238–49.
3. Iftikhar M, Usmani B, Sanyal A, Kherani S, Sodhi S, Bagheri S, et al. Progression of retinitis pigmentosa on multimodal imaging: the PREP-1 study. Clin Exp Ophthalmol. 2019;47:605–13.
4. Grover S, Fishman GA, Anderson RJ, Tozatti MSV, Heckenlively JR, Weleber RG, et al. Visual acuity impairment in patients with retinitis pigmentosa at age 45 years or older. Ophthalmology. 1999;106:1780–5.
5. Grover S, Fishman GA, Alexander KR, Anderson RJ, Derlacki DJ. Visual acuity impairment in patients with retinitis pigmentosa. Ophthalmology. 1996;103:1593–600.
6. Bainbridge JWB, Smith AJ, Barker SS, Robbie S, Henderson R, Balaggan K, et al. Effect of gene therapy on visual function in Leber's congenital amaurosis. N Engl J Med. 2008;358:2231–9.
7. MacLaren RE, Groppe M, Barnard AR, Cottriall CL, Tolmachova T, Seymour L, et al. Retinal gene therapy in patients with choroideremia: Initial findings from a phase 1/2 clinical trial. Lancet. 2014;383:1129–37.
8. Bennett J, Wellman J, Marshall KA, McCague S, Ashtari M, DiStefano-Pappas J, et al. Safety and durability of effect of contralateral-eye administration of AAV2 gene therapy in patients with childhood-onset blindness caused by RPE65 mutations: a follow-on phase 1 trial. Lancet. 2016;388:661–72.
9. Prado DA, Acosta-Acero M, Maldonado RS. Gene therapy beyond luxturna: a new horizon of the treatment for inherited retinal disease. Curr Opin Ophthalmol. 2020;31:147–54.
10. Schatz A, Röck T, Naycheva L, Willmann G, Wilhelm B, Peters T, et al. Transcorneal electrical stimulation for patients with retinitis pigmentosa: a prospective, randomized, sham-controlled exploratory study. Investig Ophthalmol Vis Sci. 2011;52:4485–96.
11. Schatz A, Pach J, Gosheva M, Naycheva L, Willmann G, Wilhelm B, et al. Transcorneal electrical stimulation for patients with retinitis pigmentosa: a prospective, randomized, sham-controlled follow-up study over 1 year. Investig Ophthalmol Vis Sci. 2017;58:257–69.
12. Busskamp V, Picaud S, Sahel JA, Roska B. Optogenetic therapy for retinitis pigmentosa. Gene Ther. 2012;19:169–75.
13. Singh MS, Charbel Issa P, Butler R, Martin C, Lipinski DM, Sekaran S, et al. Reversal of end-stage retinal degeneration and restoration of visual function by photoreceptor transplantation. Proc Natl Acad Sci USA. 2013;110:1101–6.
14. Scholl HPN, Moore AT, Koenekoop RK, Wen Y, Fishman GA, Van Den Born LI, et al. Safety and proof-of-concept study of oral QLT091001 in retinitis pigmentosa due to inherited deficiencies of retinal pigment epithelial 65 protein (RPE65) or lecithin: retinol acyltransferase (LRAT). PLoS ONE. 2015;10:e0143846.
15. Zrenner E, Bartz-Schmidt KU, Benav H, Besch D, Bruckmann A, Gabel VP, et al. Subretinal electronic chips allow blind patients to read letters and combine them to words. Proc R Soc B Biol Sci. 2011;278:1489–97.
16. Humayun MS, Dorn JD, Da Cruz L, Dagnelie G, Sahel JA, Stanga PE, et al. Interim results from the international trial of second sight's visual prosthesis. Ophthalmology. 2012;119:779–88.
17. Ayton LN, Blamey PJ, Guymer RH, Luu CD, Nayagam DAX, Sinclair NC, et al. First-in-human trial of a novel suprachoroidal retinal prosthesis. PLoS ONE. 2014;9:e115239.
18. Stingl K, Bartz-Schmidt KU, Besch D, Chee CK, Cottriall CL, Gekeler F, et al. Subretinal visual implant alpha IMS-clinical trial interim report. Vis Res. 2015;111:149–60.
19. Maya-Vetencourt JF, Ghezzi D, Antognazza MR, Colombo E, Mete M, Feyen P, et al. A fully organic retinal prosthesis restores vision in a rat model of degenerative blindness. Nat Mater. 2017;16:681–9.
20. Stingl K, Schippert R, Bartz-Schmidt KU, Besch D, Cottriall CL, Edwards TL, et al. Interim results of a multicenter trial with the new electronic subretinal implant alpha AMS in 15 patients blind from inherited retinal degenerations. Front Neurosci. 2017;11:445.
21. Edwards TL, Cottriall CL, Xue K, Simunovic MP, Ramsden JD, Zrenner E, et al. Assessment of the electronic retinal implant alpha AMS in restoring vision to blind patients with end-stage retinitis pigmentosa. Ophthalmology. 2018;125:432–43.
22. Zrenner E. Fighting blindness with microelectronics. Sci Transl Med. 2013;5:210ps16.
23. Bach M. Freiburg visual acuity & contrast test (FrACT). 2002. https://michaelbach.de/fract/index.html.
24. Schulze-Bonsel K, Feltgen N, Burau H, Hansen L, Bach M. Visual acuities "hand motion" and "counting fingers" can be quantified with the Freiburg Visual Acuity Test. Investig Ophthalmol Vis Sci. 2006;47:1236–40.
25. Lieberman HR, Pentland AP. Microcomputer-based estimation of psychophysical thresholds: The Best PEST. Behav Res Methods Instrum. 1982;14:21–5.
26. Treutwein B. Adaptive psychophysical procedures. Vis Res. 1995;35:2503–22.
27. Bach M. Anti-aliasing and dithering in the "Freiburg Visual Acuity Test.". Spat Vis. 1997;11:85–9.
28. Campochiaro PA, Mir TA. The mechanism of cone cell death in Retinitis Pigmentosa. Prog Retin Eye Res. 2018;62:24–37.
29. Punzo C, Kornacker K, Cepko CL. Stimulation of the insulin/mTOR pathway delays cone death in a mouse model of retinitis pigmentosa. Nat Neurosci. 2009;12:44–52.

30. Wang AL, Knight DK, Vu TTT, Mehta MC. Retinitis pigmentosa: review of current treatment. Int Ophthalmol Clin. 2019;59: 263–80.
31. Triolo G, Pierro L, Parodi MB, De Benedetto U, Gagliardi M, Manitto MP, et al. Spectral domain optical coherence tomography findings in patients with retinitis pigmentosa. Ophthalmic Res. 2013;50:160–4.
32. Nagasaka Y, Ito Y, Ueno S, Terasaki H. Number of hyperreflective foci in the outer retina correlates with inflammation and photoreceptor degeneration in retinitis pigmentosa. Ophthalmol Retin. 2018;2:726–34.
33. Schuerch K, Marsiglia M, Lee W, Tsang SH, Sparrow JR. Multimodal imaging of disease-associated pigmentary changes in retinitis pigmentosa. Retina. 2016;36:S147–58.
34. Aizawa S, Mitamura Y, Baba T, Hagiwara A, Ogata K, Yamamoto S. Correlation between visual function and photoreceptor inner/outer segment junction in patients with retinitis pigmentosa. Eye. 2009;23:304–8.
35. Kim YJ, Joe SG, Lee DH, Lee JY, Kim JG, Yoon YH. Correlations between spectral-domain OCT measurements and visual acuity in cystoid macular edema associated with retinitis pigmentosa. Investig Ophthalmol Vis Sci. 2013;54:1303–9.
36. Sousa K, Fernandes T, Gentil R, Mendonça L, Falcão M. Outer retinal layers as predictors of visual acuity in retinitis pigmentosa: a cross-sectional study. Graefe's Arch Clin Exp Ophthalmol. 2019;257:265–71.
37. Oster SF, Mojana F, Brar M, Yuson RMS, Cheng L, Freeman WR. Disruption of the photoreceptor inner segment/outer segment layer on spectral domain-optical coherence tomography is a predictor of poor visual acuity in patients with epiretinal membranes. Retina. 2010;30:713–8.
38. Battaglia Parodi M, La Spina C, Triolo G, Riccieri F, Pierro L, Gagliardi M, et al. Correlation of SD-OCT findings and visual function in patients with retinitis pigmentosa. Graefes Arch Clin Exp Ophthalmol. 2016;254:1275–9.
39. Cetin EN, Parca O, Akkaya HS, Pekel G. Association of retinal biomarkers and choroidal vascularity index on optical coherence tomography using binarization method in retinitis pigmentosa. Graefes Arch Clin Exp Ophthalmol. 2020;258:23–30.
40. Govetto A, Su D, Farajzadeh M, Megerdichian A, Platner E, Ducournau Y, et al. Microcystoid macular changes in association with idiopathic epiretinal membranes in eyes with and without glaucoma: clinical insights. Am J Ophthalmol. 2017;181:156–65.
41. Dolz-Marco R, Hoang QV, Gallego-Pinazo R, Chang S, ASSESSMENT OF. The significance of cystic changes after epiretinal membrane surgery with internal limiting membrane removal. Retina. 2016;36:727–32.
42. Burggraaff MC, Trieu J, de Vries-Knoppert WAEJ, Balk L, Petzold A. The clinical spectrum of microcystic macular edema. Investig Ophthalmol Vis Sci. 2014;55:952–61.
43. Abegg M, Dysli M, Wolf S, Kowal J, Dufour P, Zinkernagel M. Microcystic macular edema: Retrograde maculopathy caused by optic neuropathy. Ophthalmology. 2014;121:142–9.
44. Querques G, Kamami-Levy C, Georges A, Pedinielli A, Capuano V, Blanco-Garavito R, et al. Adaptive optics imaging of foveal sparing in geographic atrophy secondary to age-related macular degeneration. Retina. 2016;36:247–54.
45. Fleckenstein M, Mitchell P, Freund KB, Sadda SV, Holz FG, Brittain C, et al. The progression of geographic atrophy secondary to age-related macular degeneration. Ophthalmology. 2018;125: 369–90.